Pergamon

PII: S0277-5387(96)00554-2

Polyhedron Vol. 16, No. 13, pp. 2307–2313, 1997

0277-5387/97 $17.00+0.00

A water-soluble μ_2-oxo bridged diiron complex with terminally ligated iminodiacetate chelating ligands

Yong-Ge Wei, Shi-Wei Zhang* and Mei-Cheng Shao

Department of Chemistry, Peking University, Beijing 100871, P.R. China

(Received 10 September 1996; accepted 11 October 1996)

Abstract—The novel oxo-centered dinuclear iron complex $K_4[Fe_2O(IDA)_4]$ (1) (IDA = iminodiacetate) was synthesized by the air-oxidation of ferrous iron in an aqueous solution in the presence of iminodiacetate and characterized by IR, magnetic susceptibility, and X-ray crystallography methods. The structure contains dimeric units where the two crystallographically equivalent iron centers are linked by a μ_2-oxo bridge at a symmetric center of crystallography, forming a stick-like core, $[Fe_2O]^{4+}$, and have distorted octahedral environments each with one tridentate and one "bidentate-like" IDA ligands completing the coordination sphere. The iron centers are antiferromagnetically coupled in the cluster since they are bridged by the μ_2-oxo oxygen atom in the center of symmetry and this was confirmed by the magnetic susceptibility study. © 1997 Elsevier Science Ltd

Keywords: iron-oxo aggregates; dinuclear iron complex; the chemistry of iron in aqueous solution; crystal structure; antiferromagnetic coupling; magnetic properties; chelating ligands.

Binuclear oxo- and hydroxo-bridged iron complexes have recently received much attention [1,2] in biology and chemistry owing to the wide occurrence of such units in organisms and their performance of a range of biological activities such as the storage and transport of dioxygen (hemerythrin) [3], hydroxylation of alkanes (methylmonooxygenase) [4], phosphate ester hydrolysis (purple acid phosphatases) [5] and DNA synthesis (ribonucleotide reductase) [6]. Their structure, magnetic, spectroscopic and redox properties, and also chemical reactivities have been intensely investigated and are summarized in several good reviews [1,2,7–9]. Although the hydrolytic polymerization of ferric ion is a fundamental step to prepare iron-oxo/hydroxo aggregates *in vivo*, oxo-/hydroxo-bridged diiron and polyiron aggregates were obtained in laboratories before 1992 mainly by the hydrolysis of ferric salts in nonaqueous solvent in the presence of carboxylate since the hydrolysis is rather difficult to control in an aqueous solution, which usually forms iron(III) hydroxide, $Fe(OH)_3$, a polymeric oxo-/hydroxo- bridged iron(III) species. However, the work reported recently by Powell *et al.* [10–12] implies that in an aqueous solution, the hydrolysis of ferric salts *in vitro* might be controlled in the individual steps and the resulting oligomeric iron-oxo clusters can be isolated in conjunction with chelating ligands in favourable cases. In the course of our studies on the magnetostructural relationships in oxo-bridged polymetal clusters in order to design novel molecular magnetic materials, we have also examined the hydrolytic polymerization and oxidation reactions of ferrous salts in aqueous solution in the presence of chelating ligands. The present study is concerned with the iminodiacetate ligand and herein are reported the structure, infra-red spectroscopy and magnetic property of a dinuclear complex of this ligand, $K_4[Fe_2O(IDA)_4]$.

*Author to whom correspondence should be addressed. E-mail: zhangsw@pschnetware.pku.edu.cn

EXPERIMENTAL

Preparation of $K_4[Fe_2O(IDA)_4]\cdot 10H_2O$

$FeCl_2\cdot 4H_2O$ (0.6 g, 3 mmol) was added with constant stirring into a solution of iminodiacetic acid (1.2 g, 9 mmol) and KOH (1.1 g, 19.5 mmol) in water (10 cm^3). After five min, a light red solution was given

and the colour of the solution became more and more dark with the continuation of the reaction. The resulting dark red solution with pH = *ca* 8 was allowed to filter in about half an hour. Open to the air without disturbance, rhombohedral red crystals suitable for X-ray diffraction were deposited in about 50% yield based on iron from the filtrate in 3 days. The crystals lost solvent molecules quickly on being exposed to air. Found: C, 19.8; H, 3.5; N, 5.6; K, 15.8; Fe, 11.1. Calc. for $C_{16}H_{36}N_4O_{25}K_4Fe_2$: C, 20.2; H, 3.8; N, 5.9; K, 16.4; Fe, 11.7%.

X-ray crystallography

Crystallographic data $K_4[C_{16}H_{20}N_4O_{17}Fe]\cdot 10H_2O$ 988.6, monoclinic, space group $P2_1/c$, $a = 11.124(2)$, $b = 17.165(4)$, $c = 9.560(2)$ Å, $\beta = 105.89(1)°$, $U = 1755.8(6)$ Å^3, $Z = 2$, $D_c = 1.870$ Mg m^{-3}, $F(000) = 1016$, μ(Mo-K_α) = 1.401 mm^{-1}.

Data collection and processing. A dark red crystal of approximate size 0.2 × 0.2 × 0.3 mm was mounted in a sealed capillary and used to collect diffraction data at 22°C on an R3m/V four-circle diffractometer with graphite monochromated Mo-K_α radiation, $\lambda = 0.71073$ Å. Diffractometer control software P3R3 version 4.1 for VAX VMS system was supplied by Siemens Analytical Instruments, Inc. Cell parameters were refined by a least-squares procedure on 25 reflections in the range $\theta = 5$–12.5°. The $\theta/2\theta$ scan technique in a variable scan speed from 4.99–29.3° per min was employed to measure the intensities of a total of 3,458 reflections up to a maximum Bragg angle of 25°. Three standard reflections were monitored every 100 reflections throughout the measurement in the intensity cut-off less than 3% and no decay of the crystal was observed during data collection. The space group, $P2_1/c$, was established unambiguously by the systematic absences of the intensity data. All the data were corrected for Lorentz and polarization effects and semiempirical absorption correction [13] was also made according to experimental ψ scan curves for three reference reflections: $T_{max} = 1.000$ and $T_{min} = 0.8839$. However, no correction was applied to the data for extinction. There were 3101 independent reflections with $R_{int} = 0.0067$, of which 2820 reflections satisfying $F \geqslant 4.0\sigma(F)$ criterion of observability were used in subsequent analysis.

Structure solution and refinement. All the Fe and K atoms were located by direct methods and the remaining non-hydrogen atoms were located in successive iterations of full-matrix least-squares refinement and F and difference Fourier syntheses. In addition to half of the Fe_2 anionic cluster and two K^+ ions, the asymmetric unit was found to contain six peaks [Ow(1) through Ow(5) and Ow(5′)] of solvent that could be interpreted as H_2O molecules in the lattice; two of them [Ow(5) and Ow(5′)] were disordered and were assigned 50% occupancy in the refinement. Furthermore, there were 17 hydrogen atoms except for the five H atoms on water molecules Ow(4), Ow(5) and Ow(5′) located in the asymmetric unit which were clearly visible in the difference Fourier maps. All non-hydrogen atoms were refined with anisotropic thermal parameters and the located hydrogen atoms were isotropically refined in the final cycles. A weighting scheme $w^{-1} = \sigma^2(F) + 0.001\sigma^2(F)$ was used during the final cycles of refinement and the refinement converged with a maximum Δ/σ of 0.002 when $R = 0.0461$, $wR = 0.0634$ and goodness-of-fit = 1.71 based on 2820 observed reflections for 318 variables. The largest residual peak and hole of electron density in the final difference Fourier map were 0.65 and −1.01 e Å^{-3}, respectively, both in the vicinity of the metal atoms.

Atomic scattering factors and anomalous dispersion corrections for all atoms were taken from the usual source [14]. All the calculations were performed with the SHELXTL PLUS software package [15] on a digital Equipment Corp. MicroVAX-II computer.

Infra-red spectroscopy and magnetic susceptibility measurement

The IR spectrum of this compound was recorded in the scan range from 200 to 4000 cm^{-1} on a Perkin-Elmer 983-G IR spectrophotometer on KBr discs at room temperature.

Solid state magnetic measurement of a polycrystalline powder sample sealed in vaseline was performed with a CF-1 type extracting sample magnetometer at 70 KOe over the temperature range 2–300 K. The diamagnetism has been corrected.

RESULTS AND DISCUSSION

Synthesis

The chemistry of iron(II) with iminodiacetic acid in an aqueous solution is rather complicated. Various products are formed under favourable reaction conditions. The pH of the solution affects the product formed. The product which forms at low pH *ca* 2–3 is a polymeric compound [16] of iron with iminodiacetate. At higher pH *ca* 4–8, the dimeric $[Fe_2O(IDA)_4]^{4-}$ and other oligomeric products [17] such as $[Fe_6O_2(OH)_6(IDA)_6]^{4-}$ form and once the pH exceeds about 9, a mixture of ferric and ferrous hydroxide is obtained. Also, the concentration of the ligand affects the species formed. Solutions containing Fe^{2+} and IDA^{2-} in a 1 : 3 mole ratio yield the dimeric cluster anion up to pH = 8 as discussed above. Below this ratio, for example in a 1 : 4 ratio, the mononuclear complex [17] $[Fe(IDA)_2]^-$ forms even from solutions of pH = 10, demonstrating the ability of excess ligand to prevent iron from being hydrolysed. With a 1 : 2 ratio the hexameric complex $[Fe_6O_2(OH)_6(IDA)_6]^{4-}$ could be stabilized in solutions of pH range 4–7.5. However, above this ratio such as a 1 : 1 ratio

a polymeric cluster [16] in solutions of pH = 2–6 will precipitate in several hours or even several days depending on the specific pH of the solution.

Structure description

Crystals of $K_4[Fe_2O(IDA)_4]\cdot 10H_2O$ are made of potassium ions, discrete diiron cluster anions, $[Fe_2O(IDA)_4]^{4-}$, and water of crystallization. Figure 1 shows an ORTEP drawing of the structure of the cluster anion together with the numbering scheme used. And Fig. 2 is a packing illustration of the unit cell. Some selected bond lengths and angles are given in Tables 1 and 2, respectively.

In the anion there are two crystallographically equivalent iron atoms which are coordinated in a distorted octahedral arrangement each to an N_2O_4 donor set. The geometry deviates from octahedral with bond angles ranging from 76.5(1) [O(1)—Fe—N(1)] to 104.0(1)° [O(5)—Fe—O(9)]. The distorted octahedral N_2O_4 donor set is composed of a μ_2-oxo oxygen atom O(9) located in the crystallographic center of symmetry, a tridentate iminodiacetic acid ligand N(1), O(1) and O(3), and another iminodiacetate only supplied two coordination atoms N(1) and O(5). Although the cluster was obtained from ferrous reagent, the iron is still tervalent because there are four charge-compensating counterions K^+ in the complex and it is also confirmed by the bond-valence-sum analysis [18] which implies that iron atoms in this cluster have a valency of 2.9. For singly μ_2-oxo-bridged binuclear iron(III) complexes, the most favourable arrangement is expected to be linear if there are no crystal-packing forces. In this dimer the Fe—O(9)—FeA angle is exactly 180° by symmetry. As in other $[Fe_2O]^{4+}$ aggregates, the Fe—O bonds in the bridge are significantly shorter than the Fe—O (carboxylate) bonds. The Fe—O(9) bond distance of 1.798(1) Å also lies at the extreme end of the range 1.73–1.82 Å reported for other $[Fe_2O]^{4+}$ clusters [7]. However, the Fe—Fe distance of 3.596(1) Å is slightly longer than the highest value of 3.563(1) Å found in other symmetric μ_2-oxo monobridged diiron complexes [7]. The Fe—N(1) bond length of 2.286(3) Å is longer than that of Fe—N(2) (2.186 Å) owing to the *trans*-influence since N(1) is located *trans* to the μ_2-oxo bridge O(9) which is strongly coordinated to the iron center. In addition, both the Fe—N distances are significantly longer than the Fe—O bond lengths, which may result from the greater affinity of iron for oxygen than for nitrogen. This has been observed for other complexes of mixed N—O donating ligands [10].

The potassium ions which keep charge balance in the complex are grouped into two sets which both

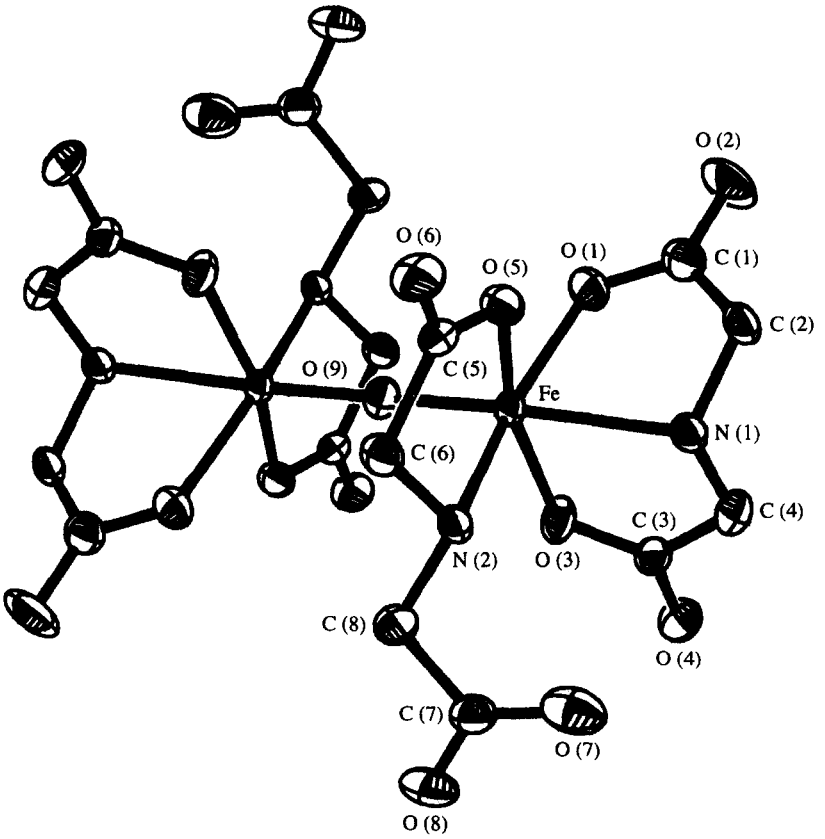

Fig. 1. An ORTEP drawing of the cluster anion $[Fe_2O(IDA)_4]^{4-}$ showing the atomic numbering scheme.

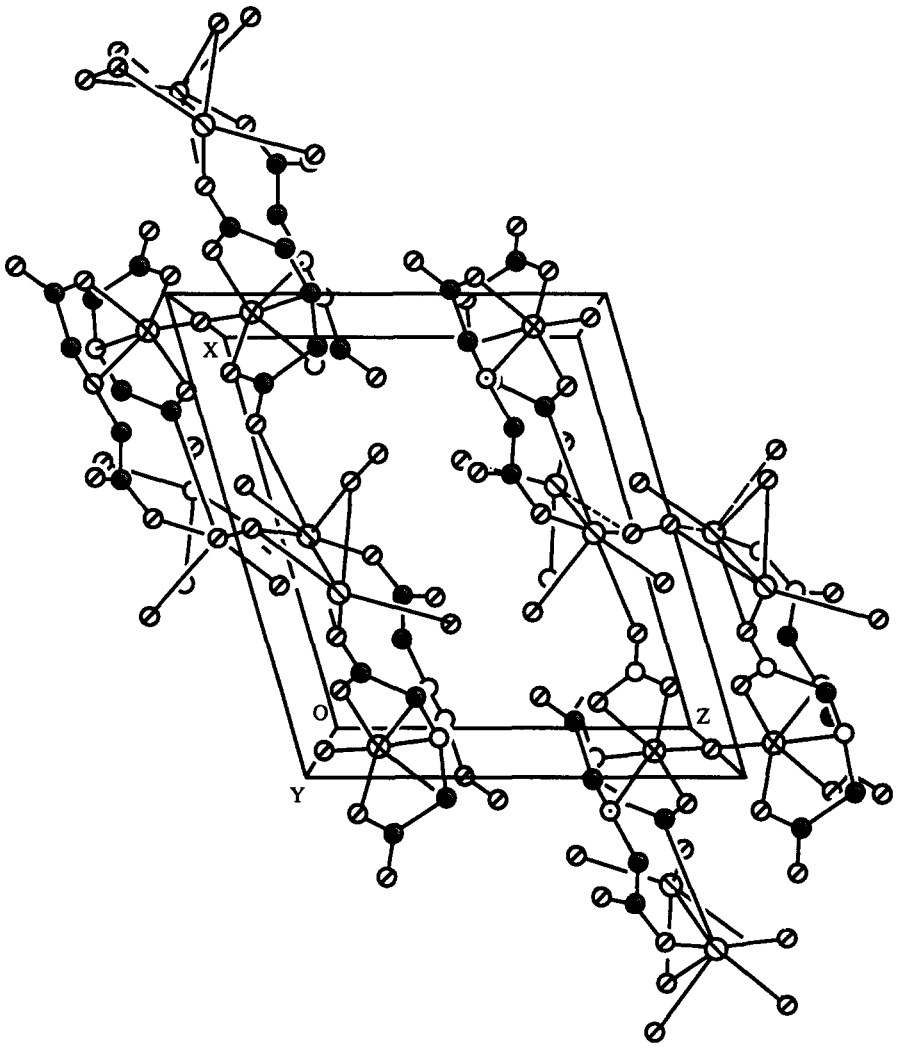

Fig. 2. Packing of $K_4[Fe_2O(IDA)_4]\cdot 10H_2O$ in a unit cell.

Table 1. Selected bond distances (Å)

Fe—O(1)	2.036(2)	Fe—O(3)	2.015(3)
Fe—O(5)	2.088(3)	Fe—O(9)	1.798(1)
Fe—N(1)	2.286(3)	Fe—N(2)	2.186(3)
K(1)—O(4)	2.672(3)	K(1)—Ow(3)	2.660(4)
K(1)—Ow(4)	2.878(5)	K(1)—Ow(5)	2.745(10)
K(1)—O(6A)	2.845(3)	K(1)—O(7A)	2.794(3)
K(1)—O(8A)	2.919(3)	K(2)—O(4)	2.767(3)
K(2)—O(8)	3.068(3)	K(2)—Ow(1)	2.918(3)
K(2)—Ow(2)	2.711(5)	K(2)—Ow(4)	2.792(5)
K(2)—Ow(5)	2.833(8)	K(2)—Ow(5′)	2.803(11)
K(2)—O(2A)	3.179(3)	K(2)—Ow(3A)	2.759(4)
K(2)—Ow(5A)	2.904(11)		

have unusual nearest oxygen atom environments [19]; one set K(1) lies within 3.2 Å of only seven oxygen atoms, which consist of three lattice water molecules and four carboxylate oxygen atoms derived from two ligands, with distances ranging from 2.660(4) to 2.919(3) Å. The other set K(2) is surrounded by ten oxygen atoms within 3.2 Å, comprised of seven water molecules of crystallization and three carboxylate oxygen atoms of three iminodiacetates with distances in the range 2.711(5)–3.179(3) Å. Apparently, these

Table 2. Selected bond angles (°)

O(1)—Fe—O(3)	95.9(1)	O(1)—Fe—O(5)	86.7(1)
O(3)—Fe—O(5)	160.4(1)	O(1)—Fe—O(9)	101.0(1)
O(3)—Fe—O(9)	94.6(1)	O(5)—Fe—O(9)	104.0(1)
O(1)—Fe—N(1)	76.5(1)	O(3)—Fe—N(1)	77.5(1)
O(5)—Fe—N(1)	84.2(1)	O(9)—Fe—N(1)	171.3(1)
O(1)—Fe—N(2)	159.3(1)	O(3)—Fe—N(2)	95.9(1)
O(5)—Fe—N(2)	76.6(1)	O(9)—Fe—N(2)	95.0(1)
N(1)—Fe—N(2)	89.5(1)		

potassium ions and diiron cluster anions as well as lattice water molecules are held together by electrostatic forces to form the present crystal. The packing of them in a unit cell is shown in Fig. 2.

Infrared spectrum

As shown in Fig. 3, the infrared spectrum of this complex shows two strong features at *ca* 1380 and 1598 cm^{-1}, assigned to ν_s(COO) and ν_{as}(COO), respectively. Both the features lie on the extreme values found for metal complexes with monodentate carboxylates [ν_s(COO) and ν_{as}(COO) in respective ranges 1267–1380 cm^{-1} and 1600–1725 cm^{-1}] [20]. Furthermore, the difference $\Delta\nu = 218$ cm^{-1} between these two features is also in agreement with the case for monodentate coordination [20]. Another strong absorption of the spectrum is in the region from 3600 to 3000 cm^{-1} and this broad band originates from the OH stretching vibrations of lattice water molecules. In addition, the Fe—O—Fe antisymmetric stretch is clearly visible at 838 cm^{-1} as a sharp peak.

Magnetochemistry

The variable-temperature (2–300 K) magnetic susceptibility data were collected for a polycrystalline sample of $\mathbf{1}\cdot 10H_2O$ in order to investigate the magnetic properties of this complex. The sample was sealed in vaseline to prevent any efflorescing of the crystals in air and a strong magnetic field up to 70 KOe was applied due to rather weak magnetization of this sample. The variations of molar magnetic susceptibility (χ_M) and effective magnetic moment per molecule (μ_{eff}) with temperature for this complex are illustrated in Fig. 4. As can be seen in Fig. 4, the μ_{eff} for $\mathbf{1}\cdot 10H_2O$ at 299 K is only 2.86 μ_B and it goes down steadily with decreasing temperature to 0.62 μ_B at 2 K, which implies that there is strong antiferromagnetic coupling interactions between the two iron centers in

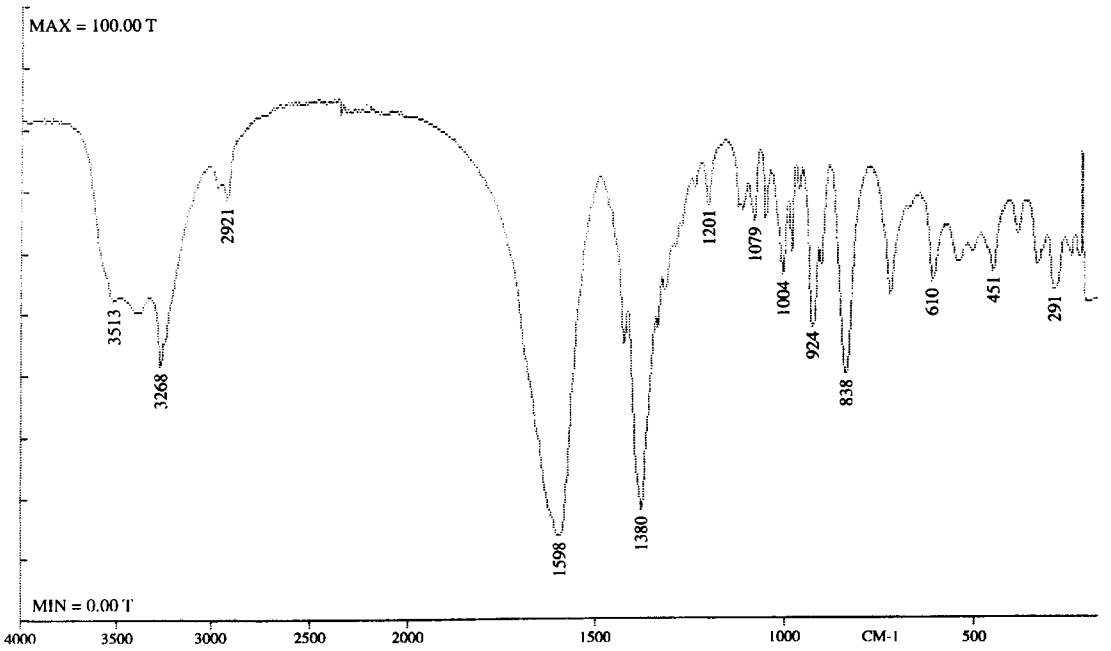

Fig. 3. Infrared spectrum of $K_4[Fe_2O(IDA)_4]\cdot xH_2O$.

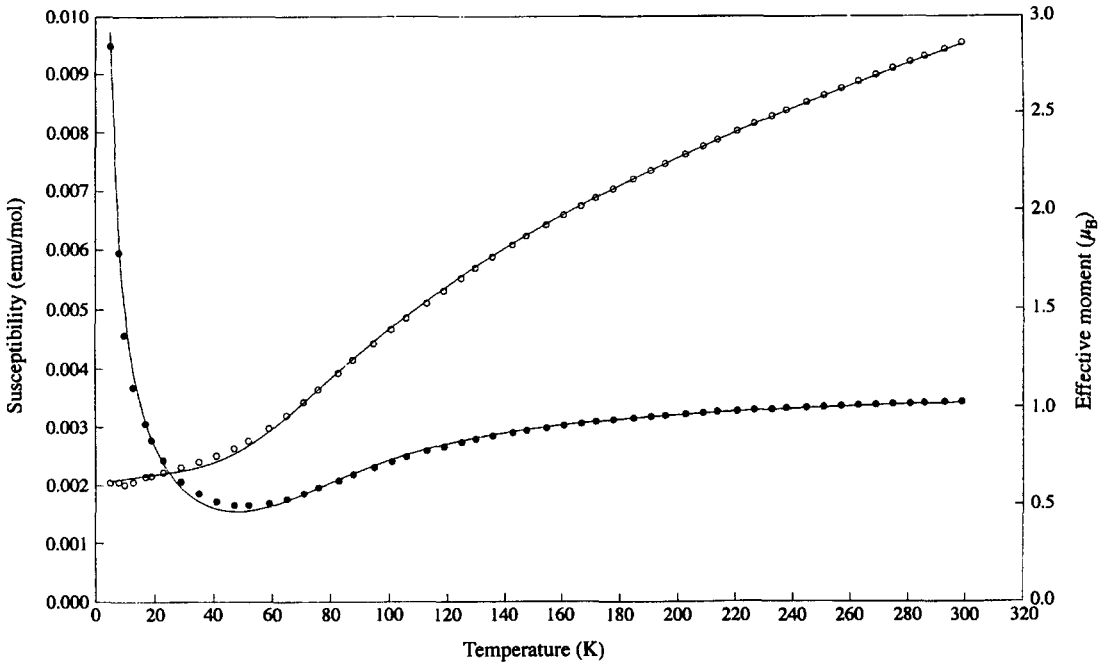

Fig. 4. Molar magnetic susceptibility data and effective magnetic moment *vs* temperature for a polycrystalline sample of $\mathbf{1}\cdot 10H_2O$. The solid lines result from a nonlinear least-squares fitting to the theoretical expression.

cluster 1. In addition, the susceptibility goes up with decreasing temperature below *ca* 50 K, which suggests that there are some paramagnetic impurities such as the monomeric Fe^{3+}.

In order to acquire a quantitative result on the magnetic property of $\mathbf{1}\cdot H_2O$. Analysis of the susceptibility data has also been carried out using the isotropic Heisenberg-Dirac-van Vleck model with the following spin Hamiltonian [21] which involves coupling constant J,

$$H = -2JS_1 \cdot S_2, \tag{1}$$

where $S_1 = S_2 = 5/2$ for Fe^{3+} center, by the use of the van Vleck equation [22] with the eigenvalues of the above spin-coupling Hamiltonian as follows

$$E_S = -J[S(S+1) - S_1(S_1+1) - S_2(S_2+1)] \tag{2}$$

where $S = |S_1 - S_2|, |S_1 - S_2 + 1|, \ldots, S_1 + S_2$. This gives rise to [21]

$$\chi'_M = \frac{Ng^2\mu_B^2(2e^{2x} + 10e^{6x} + 28e^{12x} + 60e^{20x} + 110e^{30x})}{KT(1 + 3e^{2x} + 5e^{6x} + 7e^{12x} + 9e^{20x} + 11e^{30x})} \tag{3}$$

where χ'_M is the molar magnetic susceptibility and $x = J/kT$. The fit of the data to the van Vleck equation was improved by the addition of a small amount of monomeric high-spin Fe^{3+} impurity. Thus eq. (3) was modified in the following manner:

$$\chi_M = (1-P)\chi'_M + 2P\chi_c + TIP, \tag{4}$$

where χ_M is the total calculated susceptibility, χ'_M is the spin-coupled susceptibility calculated form eq. (3), χ_c is the Curie law magnetic susceptibility defined by

$$\chi_c = Ng^2\mu_B^2 S(S+1)/3kT \tag{5}$$

for the monomeric Fe^{3+} with $S = 5/2$ impurity, and *TIP* stands for the temperature independent paramagnetism.

Nonlinear least-squares fitting of the above-mentioned model to the experimental data has been made by varying J, g, P, and *TIP* and minimizing the residual $R = [\Sigma(\chi_{obs} - \chi_{calc})^2/\Sigma(\chi_{obs})^2]^{1/2}$. And very good agreement between theory and experimental data was obtained by using the following parameters: $g = 1.92$, $J = -93.2$ cm^{-1}, $P = 0.58\%$, and $TIP = 3.4 \times 10^{-4}$ (Fig. 3) with residual $R = 8.2 \times 10^{-4}$.

Obviously, the resulting J value is consistent with those obtained from other μ_2-oxo monobridged diiron complex [7]. It also implies that the present diiron complex has an $S = 0$ spin ground state with strongly antiferromagnetic interactions between these two iron centers according to eq. (2). In fact, this kind of magnetic characteristic originates from the topological structure arrangement of this cluster however. According to our knowledge, the interactions between two iron centers in binuclear clusters must be antiferromagnetic if they are surrounded by vertex-sharing or edge-sharing polyhedra and it seems that the interactions can be enhanced if there are symmetric centers in such clusters [7]. Furthermore, there are only three ferromagnetic coupling diiron complexes reported in the literature [23–25] where the iron cen-

ters are surrounded by the face-sharing octahedra, which seem to be in favor of the ferromagnetic interactions between metal centers. These magnetostructural relationships maybe helpful to the design of large spin ground state molecules and novel molecular ferromagnets.

Acknowledgements—This work was supported by the National Natural Science Foundation of China, the Key Project in Climbing Program from the State Science and Technology Commission and the Doctoral Foundation of the State Educational Committee. We thank Professor Wen-Sheng Zhou for helpful discussions in magnetism and Ms Hong-Li Tu for typing this manuscript.

REFERENCES

1. Que, L., Jr and True, A. E., *Prog. Inorg. Chem.* 1990, **38,** 97.
2. Sanders-Loehr, J., in *Iron Carriers and Iron Proteins* (Edited by T. M. Loeher), p. 373. VCH, New York (1989).
3. (a) Holmes, M. A. and Stenkamp, R. E. *J. Mol. Biol.* 1991, **220,** 723; (b) Stenkamp, R. E., Sieker, L. C. and Jensen, L. H., *J. Am. Chem. Soc.* 1984, **106,** 618.
4. Rosenzweig, A. C., Frederick, C. A., Lippard, S. J. and Norlund, P., *Nature* 1993, **366,** 537.
5. True, A. E., Scarrow, R. C., Randall, C. R., Holz, R. C. and Que, L. Jr, *J. Am. Chem. Soc.* 1993, **115,** 4246.
6. Nordlund P. and Eklund, H., *J. Mol. Biol.* 1993, **232,** 123.
7. Kurtz, D. M. Jr, *Chem. Rev.*, 1990, **90,** 585.
8. Vincent, J. B., Olivier-Lilley, G. L. and Averill, B. A., *Chem. Rev.* 1990, **90,** 1447.
9. Wilkins, P. C. and Wilkins, R. G., *Coord. Chem. Rev.* 1987, **7,** 195.
10. Heath, S. L., Powell, A. K., Utting H. L. and Helliwell, M., *J. Chem. Soc., Dalton Trans.* 1992, 305 and references cited therein.
11. Heath, S. L. and Powell, A. K., *Angew. Chem., Int. Ed. Engl.* 1992, **31,** 191.
12. Harding, C. J., Henderson R. K. and Powell, A. K., *Angew. Chem. Int. Ed. Engl.* 1993, **32,** 570.
13. North, A. C. T., Phillips, D. C. and Mathews, M. S., *Acta Cryst.* 1968, **A24,** 351.
14. International Tables for X-ray Crystallography, Vol. IV. Kynoch Press, Birmingham (1974).
15. Sheldrick, G., *SHELXTL-PLUS Program for Crystal Structure Refinement.* Institüt für Anorganische Chemie der Universität, Gottingen, Germany (1990).
16. Wei, Y. G. and Zhang, S. W., unpublished work.
17. Wei, Y. G. and Zhang, S. W., submitted to *Acta Cryst., Sect C.*
18. Brown, I. D. and Altermatt, D., *Acta Cryst.* 1985, **B41,** 244.
19. Wei, Y. G., Zhang, S. W., Huang, G. Q. and Shao, M. C., *Polyhedron* 1994, **13,** 1587.
20. Nakamoto, K., *Infrared and Raman Spectra of Inorganic and Coordination Compounds*, 4th edn., p. 231. Wiley, New York (1986).
21. O'Connor, C. J., *Prog. Inorg. Chem.* 1979, **29,** 204.
22. van Vleck, J. H., *The Theory of Electric and Magnetic Susceptibilities.* Reprinted by Lowe, Oxford University Press, London (1954).
23. Dance, J. M., Mur, J., Darriet, J., Hagenmuller, P., Massa, W., Kummer, S. and Babel, D., *J. Sol. State Chem.* 1986, **63,** 446.
24. Drüeke, S., Chaudhuri, P., Pohl, K., Wieghardt, K., Ding, X.-Q., Bill, E., Sawaryn, A., Trautwein, A. X., Winkler, H. and Gurman, S. J., *J. Chem. Soc., Chem. Commun.*, 1989, 59.
25. Shweky, I., Bino, A., Goldberg, D. P. and Lippard, S. J., *Inorg. Chem.* 1994, **33,** 5161.